Eur. Phys. J. C 44, 375–382 (2005)
Digital Object Identifier (DOI) 10.1140/epjc/s2005-02368-8

THE EUROPEAN PHYSICAL JOURNAL C

The production of ρ, ω and ϕ vector-mesons by protons and sulphur ions with incident momentum of 200 GeV/c per nucleon

The NA38 Collaboration

M.C. Abreu[4,a], J. Astruc[5], C. Baglin[1], A. Baldit[2], M. Bedjidian[7], P. Bordalo[4,b,f], G. Borges[4], A. Bussière[1], J. Castor[2], B. Chaurand[6], I. Chevrot[2], B. Cheynis[7], A. Devaux[2], O. Drapier[7,c], B. Espagnon[2], J. Fargeix[2], R. Ferreira[4], P. Force[2], C. Gerschel[5], J.Y. Grossiord[7], A. Guichard[7], J. Guimarães[4,d], R. Haroutunian[7], D. Jouan[5], L. Kluberg[6], C. Lourenço[3], S. Mourgues[2], P. Petiau[6], J.R. Pizzi[7], C. Quintans[4], S. Ramos[4,b], A. Romana[6], H. Santos[4], P. Saturnini[2], R. Shahoyan[4,e], P. Sonderegger[3,b], X. Tarrago[5]

[1] LAPP, CNRS-IN2P3, Annecy-le-Vieux, France
[2] LPC, Université Blaise Pascal and CNRS-IN2P3, Aubière, France
[3] CERN, Geneva, Switzerland
[4] LIP, Lisbon, Portugal
[5] IPN, Université de Paris-Sud and CNRS-IN2P3, Orsay, France
[6] LLR, Ecole Polytechnique and CNRS-IN2P3, Palaiseau, France
[7] IPN, Université Claude Bernard Lyon-I and CNRS-IN2P3, Villeurbanne, France

Received: 27 May 2005 / Revised version: 26 July 2005 /
Published online: 11 October 2005 –

Abstract. The production of ρ, ω and ϕ vector-mesons, detected through their $\mu\mu$ decay channel, is studied in p-W, S-S, S-Cu and S-U reactions at 200 GeV/c per nucleon incident momentum. Their inclusive cross-sections are determined in various transverse momentum intervals and their dependence on the projectile and target mass numbers is investigated. The relative yield $B_{\mu\mu}\sigma_\phi/(B_{\mu\mu}\sigma_\rho+B_{\mu\mu}\sigma_\omega)$ is measured, both as a function of the transverse momentum, p_T, and of the collision centrality. While this ratio exhibits no significant dependence with p_T, it clearly increases with the centrality of the collision. Effective temperatures deduced from the transverse mass spectra, $d\sigma/dM_T$, lead to values of $T_{\rho+\omega}$ equal or slightly higher than T_ϕ. Both these effective temperatures smoothly increase from p-W to S-U reactions.

1 Introduction

The NA38 Experiment has studied the production of muon pairs in ultra-relativistic heavy ion collisions. The original motivation was the prediction that prompt dimuons emitted from these collisions are a potential probe for the phase transition from ordinary nuclear matter to a new state of deconfined quarks and gluons, the so-called quark-gluon plasma or QGP [1]. Among other QGP signatures, an over-production of $s\bar{s}$ pairs is expected in this new state, leading to an enhanced production of strange particles [2], as a consequence of both (partial) chiral symmetry restoration and Pauli blocking mechanism. The ϕ meson, through its hidden strange quarks content, can also be considered as a potential probe of QGP formation [3]. The experiment has, therefore, extended its scope to the study of ϕ production which, making use of the muon detection capabilities of the detector, is easily identified through its decay into two muons. Moreover, the ϕ meson can be easily compared to similar vector-mesons built up of only light quarks, like the ρ and the ω, which are detected under identical experimental conditions and can be used as references.

2 Experimental apparatus and data collection

A detailed description of the NA38 detector can be found in [4]. For the data collected during 1991 and reported here, the experimental set-up was slightly modified in order to achieve a better muon pair mass resolution in the ϕ meson mass range and below. With this purpose, the three inner rings of the electromagnetic calorimeter, originally made of scintillating fibers embedded in a Pb converter, were replaced by a block of Al_2O_3, a good compromise for minimizing the muon multiple scattering while maximiz-

[a] also at FCT, Universidade do Algarve, Faro, Portugal
[b] also at IST, Universidade Técnica de Lisboa, Lisbon, Portugal
[c] now at LLR, Ecole Polytechnique and CNRS-IN2P3, Palaiseau, France
[d] now at Department of Physics, Harvard University, USA
[e] on leave of absence of YerPhI, Yerevan, Armenia
[f] e-mail: bordalo@lip.pt

ing, at the same time, the interaction length (in order to lower, as much as possible, the number of unwanted pion and kaon decays in the acceptance of the muon spectrometer). This modification induced a reduction of the original rapidity acceptance of the calorimeter to the range $1.7 < \eta < 2.5$, and led to a typical relative resolution in the measured transverse energy, E_T, of 4.2% for central collisions, as compared to 3.9% with the fully active calorimeter. The same material was used, instead of carbon, in the pre-absorber located upstream of the main absorber, in order to reduce the combinatorial background due to muons from pion and kaon decays. Figure 1 shows a schematic view of the target region, including the changes introduced for the collection of the data analyzed in this paper.

The spectrometer provides the muon pair trigger of the experiment and all the needed information related to the two muons. The electromagnetic calorimeter measures, on an event-by-event basis, the neutral transverse energy, E_T, released in the collision, which mainly originates from the π^0's produced in the projectile-target reaction and can be used as an experimental estimator of the collision centrality.

The target was placed between two quartz detectors, the "Beam In" (BI) and the "Beam Out" (BO) counters, both traversed by the beam. The first one was used to count the incident ions and to precisely center the beam on the targets. The second separated in-target interactions from non-interacting beam ions.

Sulphur-induced collisions are studied with this upgraded set-up, using three different targets, namely S, Cu and U. Only small samples of data were taken with the S and Cu targets, whereas a significantly larger sample was collected with the U target.

In order to increase the number of interactions detected by the experiment while, at the same time, avoiding reinteractions and potential biases due to the use of a thick target, several thin sub-targets were used, spaced 2.5 cm from each other. This target assembly was instrumented with scintillator detectors which identify the precise subtarget where the interaction takes place. In the case of S-S collisions, 21 sub-targets were used, 1.5 mm thick each, amounting to a total of 18% of an interaction length. For the S-Cu data, 12 sub-targets of the same thickness were used, corresponding to 30% of an interaction length, while the S-U assembly was made of 10 sub-targets, corresponding to 20% of an interaction length. Some preliminary results on the S-U data collected in 1991 have been already reported in [5,6]; the corresponding cross-sections are calculated and reported in the present paper. Results obtained from an older S-U data sample collected in 1990 can be found in previous publications, together with p-W results [7,8]. However, inappropriate acceptances and fit procedure used in [8] affected the $\rho+\omega$ and ϕ cross-section and effective temperature values derived in those publications, both for the p-W and S-U data. Therefore, we have updated those results in the present paper.

3 Data analysis

The data samples collected with the three different targets were reconstructed for muon pairs and further cleaned up with appropriate cuts which led to 35 000, 74 000 and 758 000 muon pair events available for the final analysis in the S-S, S-Cu and S-U samples, respectively.

The cuts applied to the data include limiting the accepted events to the laboratory rapidity window $3 < y < 4$, and to $|\cos\theta| < 0.5$ (where θ is the muon angle defined in the Collins-Soper reference frame). A low E_T cut is also applied (15 GeV for S-Cu and S-U, 7 GeV for S-S), in order to avoid spurious interactions in the BO detector located downstream from the last sub-target. Events are further selected in the dimuon transverse momentum region $0.6 < p_T < 3.0$ GeV/c, where the differential acceptances are larger than 1%.

The combinatorial background is estimated with the usual formula [8]:

$$N^{bkg} = 2\,R\,\sqrt{N^{\mu^+\mu^+}N^{\mu^-\mu^-}}\quad , \tag{1}$$

with $R = 1$, which applies provided that the parent π and K mesons are charge uncorrelated and have Poissonian multiplicity distributions. For low multiplicity events one would expect $R > 1$. As will be explained later on, the data favour $R = 1$.

In S-S collisions, the signal to background ratio varies with the muon pair transverse momentum p_T in the range 0.6 – 4.6 for the (ρ, ω) mass region and 0.5 – 3.4 for the ϕ region. For S-Cu (S-U) reactions, the corresponding variation ranges are 0.4 – 3.7 (0.3 – 2.7) and 0.4 – 2.6 (0.3 – 2.0), respectively. Following the procedure used in previous analyses [5,8,10], a detailed Monte-Carlo program is used to correct the signal event distributions for the limited acceptance and resolution of the spectrometer.

The analysis is based on a multi-dimensional deconvolution method. After generation of the dimuons mass, transverse momentum, rapidity and $\cos\theta$ distributions, an iterative procedure allows to adjust the generated distributions. Weights are applied in each kinematical bin, so that the modified distributions, tracked through the apparatus, agree with those measured for the signal.

In order to determine the different components of the dimuon invariant mass distribution (corrected for acceptance and smearing) a mass fit is performed, with the following features: three classical Breit-Wigner functions account for the vector-mesons ρ, ω and ϕ (natural widths and mean values given by the PDG [9]) and a decreasing exponential function is used to describe the continuum dominated by Dalitz decays, Drell-Yan dimuons and pairs originating from open-charm decays. More details on this method of analysis can be found in [5,8,10].

The dimuon invariant mass resolution of the spectrometer is 8% in the ϕ mass region, and 10% in the ρ and ω mass regions. It is therefore not possible to disentangle the ρ and ω resonances and treat them separately. As a consequence, all the results presented in this letter refer always to the sum of the two resonances, noted as $\rho + \omega$.

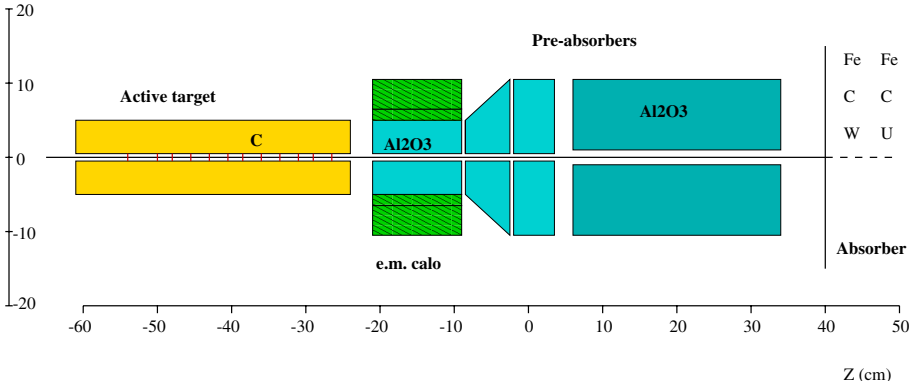

Fig. 1. The NA38 target region for the "low masses" set-up

4 Cross-sections

Cross-sections are obtained from the dimuon invariant mass distributions of the signal events, already corrected for acceptance and smearing effects, according to the expression:

$$\frac{d\sigma}{dM_{\mu\mu}} = \frac{1}{L}\,\frac{dN^{\rm signal}}{dM_{\mu\mu}}\,\frac{1}{\epsilon_{\rm trig}\;\epsilon_{\rm rec}\;\eta_{\rm reint}\;\eta_{\rm p.u.}\;\eta_{E_T}} \quad , \quad (2)$$

where L is the luminosity, $\epsilon_{\rm trig}$ and $\epsilon_{\rm rec}$ the trigger and dimuon reconstruction efficiencies and $\eta_{\rm reint}$, $\eta_{\rm p.u.}$, η_{E_T} the corrections accounting for the rejection of good events by cuts on re-interactions, interactions with piled-up incoming ions in the beam, and low E_T events, respectively. The numerical values of these quantities are given in Table 1.

A correction accounting for the inefficiency of the sub-target identification algorithm is also included [11]. This correction is performed event-by-event and is particularly severe at low E_T (for S-S, for example, this efficiency is lower than 50% for $E_T < 10$ GeV).

In each of the considered p_T intervals, the $\rho + \omega$ and ϕ cross-sections are calculated from the number of events obtained from fits to the mass spectra, corrected for acceptance and smearing, with a function of five free parameters:

$$F = P_\rho\, BW^\rho + P_\omega\, BW^\omega + P_\phi\, BW^\phi + P_4\, e^{-P_5\; M_{\mu\mu}} \quad . \quad (3)$$

The first three P parameters stand for the number of ρ, ω and ϕ events, while P_4 and P_5 adjust to the shape of the continuum. The results are presented in Tables 2 and 3 and displayed in Fig. 2, with their statistical errors only.

It is important to note that all the cross-sections quoted here are, in fact, the vector-meson production cross-sections multiplied by the corresponding branching ratios for the decay in the two muons channel, $B_{\mu\mu}$.

The systematic errors affecting these values originate from the method of analysis, namely the background subtraction and the irreducible differences between Monte-Carlo and data distributions. They also arise from uncertainties on the calculated luminosities due to the measured thickness and density of the target, the absorption of the beam in the incident beam (BI) detector, uncertainties on the efficiencies and, for proton induced reactions, pion contamination in the proton beam. These different contributions are added quadratically to obtain a total systematic error for each of the systems, as presented in Table 4.

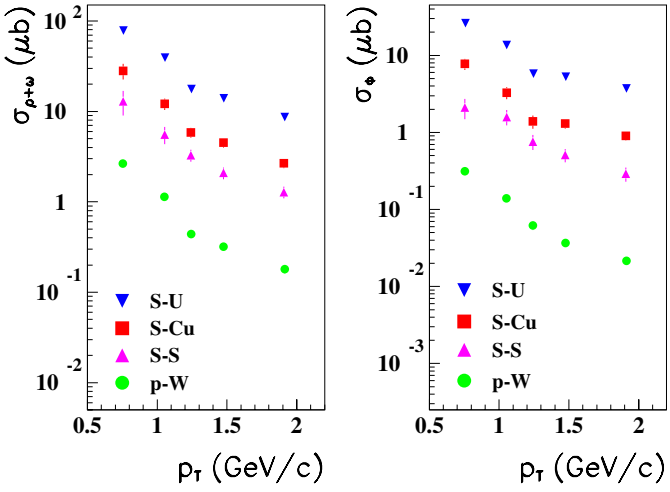

Fig. 2. Cross-sections for $\rho + \omega$ and ϕ, as a function of p_T

The background subtraction is expected to be affected by an error that depends on the transverse energy. A Monte-Carlo simulation of the background sources using the VENUS code shows that, even for very peripheral S-U collisions, the R factor in (1) is only slightly above unity, $R = 1.02$, and is compatible with unity for central collisions [12]. An experimental determination of R done by leaving R as a free parameter in the fit to the mass spectrum leads to $R = 1.06 \pm 0.03$ in the most peripheral S-U collisions [13]. A 6% increase in the R factor decreases the $\rho + \omega$ cross-section by only 2% and the ϕ cross-section by 3.5%, for the most peripheral E_T region.

We parameterize the cross-section dependence on the mass numbers of the target and projectile, A and B, by the power law:

$$\sigma = \sigma_0\,(A \times B)^\alpha \quad . \quad (4)$$

We obtain the following values for the exponents α when integrating over the full p_T range accessible to our measurements:

$$\alpha_{\rho+\omega} = 0.924 \pm 0.032(\text{stat}) \pm 0.033(\text{syst})$$

Table 1. Luminosities, efficiencies and corrections for p-W and sulphur induced reactions (luminosities already include $\epsilon_{\rm rec}$)

	p-W	S-S	S-Cu	S-U
L (b^{-1})	$(1.89 \pm 0.05)\cdot 10^{11}$	$(8.81 \pm 0.77)\cdot 10^{9}$	$(6.18 \pm 0.34)\cdot 10^{9}$	$(1.40 \pm 0.03)\cdot 10^{10}$
$\epsilon_{\rm trig}$	0.94 ± 0.06	0.94 ± 0.06	0.94 ± 0.06	0.94 ± 0.06
$\eta_{\rm p.u.}$	—	0.58	0.78	0.84
$\eta_{\rm reint}$	—	0.91	0.92	0.91
η_{E_T}	—	0.95	0.97	0.99

Table 2. Cross-sections for $\rho + \omega$ production as a function of the transverse momentum p_T, with p_T in GeV/c

$\sigma_{\rho+\omega}$ (μb)	p-W	S-S	S-Cu	S-U
$0.6 \le p_T < 0.9$	2.66 ± 0.26	13.0 ± 3.9	28.0 ± 5.5	78.2 ± 8.3
$0.9 \le p_T < 1.15$	1.14 ± 0.10	5.5 ± 1.2	12.1 ± 1.7	39.4 ± 3.2
$1.15 \le p_T < 1.35$	0.444 ± 0.039	3.27 ± 0.50	5.84 ± 0.73	17.7 ± 1.4
$1.35 \le p_T < 1.65$	0.322 ± 0.028	2.09 ± 0.31	4.51 ± 0.51	14.0 ± 1.0
$1.65 \le p_T < 3.0$	0.175 ± 0.016	1.28 ± 0.19	2.67 ± 0.32	8.66 ± 0.64
$0.6 \le p_T < 3.0$	4.92 ± 0.40	27.1 ± 5.0	51.5 ± 7.6	155.0 ± 13.0

Table 3. Cross-sections for ϕ production as a function of the transverse momentum p_T (in GeV/c)

σ_ϕ (μb)	p-W	S-S	S-Cu	S-U
$0.6 \le p_T < 0.9$	0.314 ± 0.032	2.10 ± 0.62	7.8 ± 1.3	26.2 ± 2.3
$0.9 \le p_T < 1.15$	0.140 ± 0.016	1.59 ± 0.36	3.29 ± 0.59	13.6 ± 1.2
$1.15 \le p_T < 1.35$	0.062 ± 0.008	0.76 ± 0.17	1.39 ± 0.27	5.78 ± 0.51
$1.35 \le p_T < 1.65$	0.037 ± 0.004	0.51 ± 0.10	1.30 ± 0.18	5.27 ± 0.41
$1.65 \le p_T < 3.0$	0.022 ± 0.002	0.289 ± 0.057	0.90 ± 0.12	3.72 ± 0.28
$0.6 \le p_T < 3.0$	0.569 ± 0.048	5.38 ± 0.89	14.5 ± 1.8	54.0 ± 4.0

Table 4. Total cross-sections systematic errors evaluated for proton and sulphur-induced reactions

Systematic errors (%)	$\rho + \omega$	ϕ	$\phi/(\rho + \omega)$
p-W	10.6	10.9	3.2
S-S	5.8	6.5	2.8
S-Cu	5.9	6.3	3.4
S-U	5.2	5.7	3.0

and

$$\alpha_\phi = 1.218 \pm 0.031(\text{stat}) \pm 0.032(\text{syst}).$$

As shown in Fig. 3, the exponent α increases with p_T. While $\alpha_{\rho+\omega}$ exhibits values around 1 and an increasing pattern very similar to that observed by Cronin et al. [14] for hadrons produced at 300 GeV in the same p_T range, α_ϕ is always bigger than unity, suggesting an enhanced production of (hidden) strangeness.

5 Hidden strangeness production

The enhancement of hidden strangeness production can also be studied through the ratio $B_{\mu\mu}\sigma_\phi/(B_{\mu\mu}\sigma_\rho + B_{\mu\mu}\sigma_\omega)$, abbreviated to $\phi/(\rho+\omega)$ from now on. In order to obtain this ratio, the dimuon mass spectra corrected for acceptance and smearing effects are fitted with a five free parameters function:

$$F = P_1 BW^\rho + P_1 P_2 BW^\omega + P_1 P_3 (1 + P_2) BW^\phi + P_4 e^{-P_5 M_{\mu\mu}} \quad (5)$$

where the parameters P_1, P_2 and P_3 stand for the cross-section of the ρ, and for the cross-section ratios ω/ρ and $\phi/(\rho+\omega)$ respectively. The last parameters P_4 and P_5 account for the non-resonant contributions, namely ω, η and $\eta\prime$ Dalitz decays, open charm decays and Drell-Yan pairs.

As can be seen in Table 5 and Fig. 4, the ratio $\phi/(\rho+\omega)$ increases with the mass numbers of target and projectile, but there is no significant dependence of the ratio with p_T, within the error bars, except for a slight increase observed in S-U for the highest p_T bin.

The ratio of cross-sections $\phi/(\rho+\omega)$ has also been studied as a function of centrality, with the same analysis applied independently in each of the different transverse energy bins defined in Table 6. It is worth noting that the three reactions have the same transverse energy reference, since they were taken in exactly the same experimental

Table 5. The ratio of cross-sections $\phi/(\rho+\omega)$ as a function of the transverse momentum p_T

$\phi/(\rho+\omega)$	p-W	S-S	S-Cu	S-U
$0.6 \le p_T < 0.9$	0.118 ± 0.011	0.162 ± 0.061	0.277 ± 0.060	0.335 ± 0.030
$0.9 \le p_T < 1.15$	0.123 ± 0.012	0.287 ± 0.068	0.272 ± 0.051	0.346 ± 0.023
$1.15 \le p_T < 1.35$	0.140 ± 0.016	0.233 ± 0.050	0.238 ± 0.045	0.326 ± 0.021
$1.35 \le p_T < 1.65$	0.114 ± 0.012	0.243 ± 0.045	0.289 ± 0.037	0.376 ± 0.016
$1.65 \le p_T < 3.0$	0.123 ± 0.012	0.226 ± 0.042	0.336 ± 0.040	0.429 ± 0.017

Table 6. E_T bins used for the different reactions, and corresponding mean $N_{\rm part}$ values

	S-S	S-Cu	S-U
$\Delta E_{T\ 1}$	$7. \le E_T < 22.$	$15. \le E_T < 30.$	$15. \le E_T < 46.$
$\langle N_{\rm part}\rangle_1$	19.3	28.2	40.1
$\Delta E_{T\ 2}$	$22. \le E_T < 32.$	$30. \le E_T < 44.$	$46. \le E_T < 69.5$
$\langle N_{\rm part}\rangle_2$	32.6	44.8	70.2
$\Delta E_{T\ 3}$	$32. \le E_T < 50.$	$44. \le E_T < 80.$	$69.5 \le E_T < 89.$
$\langle N_{\rm part}\rangle_3$	46.5	66.3	96.3
$\Delta E_{T\ 4}$	—	—	$89. \le E_T < 150.$
$\langle N_{\rm part}\rangle_4$	—	—	126.7

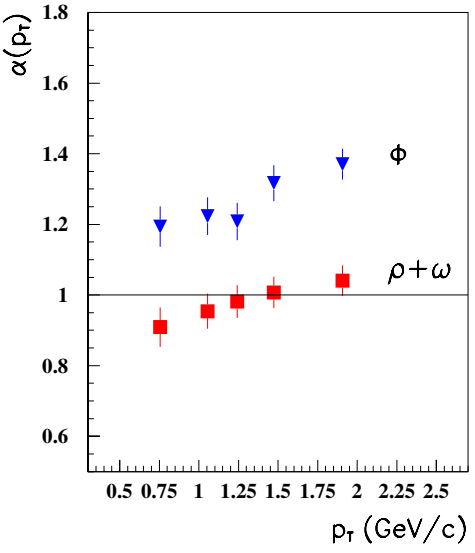

Fig. 3. A·B dependence: α as a function of p_T (obtained from p-W, S-S, S-Cu and S-U data). Statistical and systematical errors are included

Table 7. The ratio of cross-sections $\phi/(\rho+\omega)$ for different E_T bins

$\phi/(\rho+\omega)$	S-S	S-Cu	S-U
$\Delta E_{T\ 1}$	0.121 ± 0.017	0.192 ± 0.031	0.271 ± 0.020
$\Delta E_{T\ 2}$	0.194 ± 0.035	0.376 ± 0.070	0.352 ± 0.034
$\Delta E_{T\ 3}$	0.272 ± 0.054	0.206 ± 0.033	0.367 ± 0.044
$\Delta E_{T\ 4}$	—	—	0.471 ± 0.063

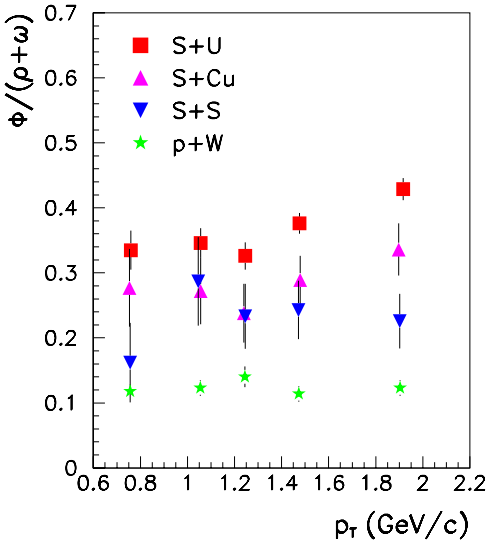

Fig. 4. The ratio $\phi/(\rho+\omega)$ as a function of p_T

conditions and in the same data taking period. Since the E_T scale is experiment dependent, the ratio is given as a function of the number of participant nucleons in the collision, $N_{\rm part}$, used here as the centrality estimator of the collision. Results are shown in Fig. 5 and Table 7.

The mean $N_{\rm part}$ value corresponding to each E_T bin is calculated from an implementation of the Glauber model [15] for each collision system, which takes into account the calorimeter resolution. In the case of p-W collisions, no electromagnetic calorimeter is used; thus the value $N_{\rm part} = 4.5$ used here is a theoretical one, obtained from the Glauber model alone.

As already reported [5], the results obtained for the two independent S-U data sets, collected first in 1990 and later in 1991 with a modified set-up, are compatible. They show a clear increase of the ratio $\phi/(\rho+\omega)$ with the centrality of the collision. The S-S and S-Cu results follow a similar dependence with $N_{\rm part}$ (Fig. 5). The errors quoted in Tables 5 and 7 are purely statistical. The estimated systematic errors are detailed in Table 4.

6 Inverse slopes of M_T distributions

The transverse mass spectra of ρ, ω and ϕ mesons, if produced in a locally equilibrated thermal medium (see [16]),

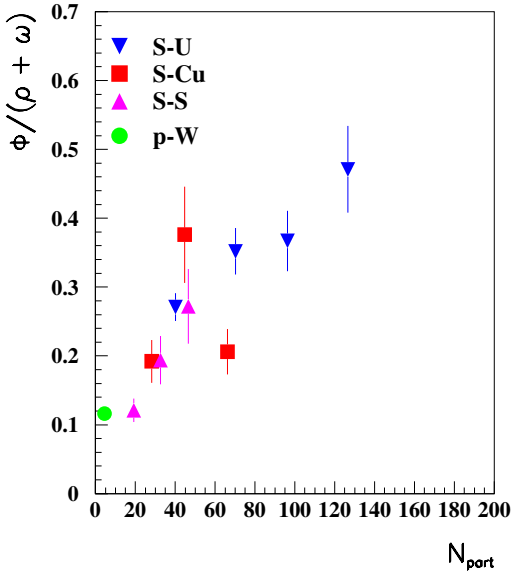

Fig. 5. The ratio of cross-sections $\phi/(\rho+\omega)$ as a function of the number of participant nucleons in the collision, $N_{\rm part}$

are expected to follow the expression:

$$\frac{d\sigma}{dM_T} \propto M_T^2 \; K_1(\frac{M_T}{T}) \qquad (6)$$

where K_1 is the modified Bessel function. If the mass of the studied resonance is significantly higher than the inverse slope parameter, T, and its p_T not too low (as is the case here), the following approximation can be used:

$$\frac{d\sigma}{dM_T} \propto M_T^{3/2} \; e^{-M_T/T} \quad . \qquad (7)$$

The number of $\rho+\omega$ and ϕ events in each of the five p_T bins is extracted from the five free parameter fit to the mass spectra (equation 3). Dividing them by the widths of the corresponding M_T regions, it is then possible to perform a two free parameter fit as a function of M_T according to

$$F \;=\; P_1 \; M_T^{3/2} \; e^{-M_T/P_2} \quad . \qquad (8)$$

The value M_T^i to be considered for bin i is such that:

$$\frac{d\sigma}{dM_T}(M_T^i) \;=\; \frac{\int_{\Delta M_T} \frac{d\sigma}{dM_T} \; dM_T}{M_{T_2}^i - M_{T_1}^i} \quad . \qquad (9)$$

Results are presented in Tables 8 and 9 and in Fig. 6. The systematic errors are taken into account in these fits, since they affect differently each M_T point. The temperature increases with A·B, as expected. $T_{\rho+\omega}$ is equal or slightly higher than T_ϕ.

Table 8. $\rho+\omega$ differential cross-section as a function of M_T, in p-W, S-S, S-Cu and S-U systems

$\rho+\omega$	p-W				
M_T (GeV/c^2)	1.08	1.28	1.47	1.68	2.23
$d\sigma/dM_T$ ($\mu b \cdot c^2$/GeV)	12.88 ± 1.84	5.72 ± 0.80	2.61 ± 0.36	1.21 ± 0.16	0.14 ± 0.02
	S-S				
M_T (GeV/c^2)	1.08	1.28	1.47	1.68	2.24
$d\sigma/dM_T$ ($\mu b \cdot c^2$/GeV)	62.59 ± 18.95	27.82 ± 5.97	19.24 ± 2.93	7.87 ± 1.16	1.00 ± 0.15
	S-Cu				
M_T (GeV/c^2)	1.08	1.28	1.47	1.68	2.25
$d\sigma/dM_T$ ($\mu b \cdot c^2$/GeV)	135.36 ± 26.62	60.85 ± 8.64	34.37 ± 4.31	16.94 ± 1.93	2.09 ± 0.25
	S-U				
M_T (GeV/c^2)	1.08	1.28	1.47	1.68	2.25
$d\sigma/dM_T$ ($\mu b \cdot c^2$/GeV)	77.72 ± 40.22	198.08 ± 16.23	104.26 ± 8.07	52.64 ± 3.89	6.79 ± 0.50

Table 9. Same as previous table, for the ϕ meson

ϕ	p-W				
M_T (GeV/c^2)	1.27	1.44	1.61	1.80	2.32
$d\sigma/dM_T$ ($\mu b \cdot c^2$/GeV)	1.76 ± 0.29	0.80 ± 0.13	0.40 ± 0.07	0.15 ± 0.02	0.02 ± 0.00
	S-S				
M_T (GeV/c^2)	1.27	1.44	1.61	1.81	2.34
$d\sigma/dM_T$ ($\mu b \cdot c^2$/GeV)	11.80 ± 3.49	9.02 ± 2.03	4.93 ± 1.11	2.05 ± 0.41	0.24 ± 0.05
	S-Cu				
M_T (GeV/c^2)	1.27	1.44	1.61	1.81	2.35
$d\sigma/dM_T$ ($\mu b \cdot c^2$/GeV)	43.55 ± 7.23	18.72 ± 3.36	8.97 ± 1.76	5.26 ± 0.74	0.73 ± 0.09
	S-U				
M_T (GeV/c^2)	1.27	1.44	1.61	1.81	2.35
$d\sigma/dM_T$ ($\mu b \cdot c^2$/GeV)	147.36 ± 13.08	77.50 ± 6.73	37.29 ± 3.30	21.26 ± 1.64	3.02 ± 0.22

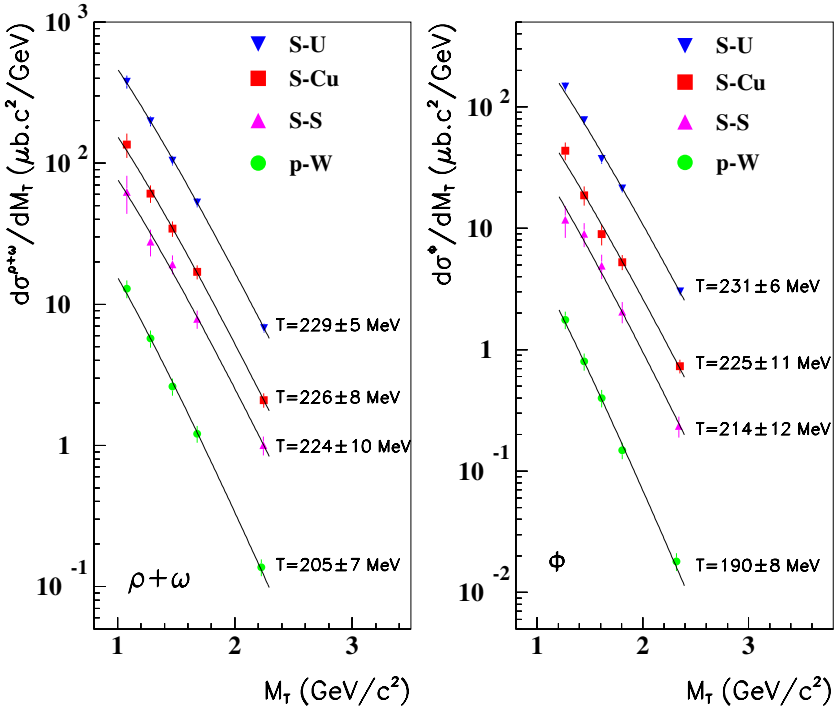

Fig. 6. Differential cross-sections for $\rho+\omega$ and ϕ as a function of the transverse mass, in the p-W, S-S, S-Cu and S-U collision systems

In the non-relativistic domain, where $p_T \ll m_R$ (m_R being the resonance mass), the inverse slope parameter depends both on the freeze-out temperature, T_f, and on the collective motion velocity, v_T, according to (see [17], for example): $T = T_f + m_R \frac{<v_T>^2}{c^2}$, while in the relativistic domain ($p_T \gg m_R$) there is a blue-shifted dependence on T_f and the inverse slope parameter, expected to be the same for all particles, is given by: $T = T_f \sqrt{\frac{1+<v_T>}{1-<v_T>}}$. In our case, the p_T region studied is somewhere between these two extreme limits ($0.6 < p_T < 3.0$ GeV/c). Temperatures for $\rho+\omega$ and for ϕ are already very similar, and their rise when going from proton to sulphur induced reactions is probably due both to an increase of the produced energy density and to the collective transverse motion of the source.

7 Conclusions

We have studied ρ, ω and ϕ production in p-W, S-S, S-Cu and S-U reactions at 200 GeV/nucleon incident momentum, as a function of the transverse momentum and of the centrality. The ratio of cross sections $\phi/(\rho+\omega)$ increases by a factor of 5 from p-W up to the most central S-U collisions. When the cross-sections are parameterized as a function of the mass numbers of projectile and target according to $(A \cdot B)^\alpha$ we find, in the transverse momentum range 0.6 – 3.0 GeV/c, exponent average values of $\alpha_{\rho+\omega} = 0.924 \pm 0.032(\text{stat}) \pm 0.033(\text{syst})$ and $\alpha_\phi = 1.218 \pm 0.031(\text{stat}) \pm 0.032(\text{syst})$ and, in both cases, a clear increase with increasing transverse momentum. The inverse slopes of the dimuon transverse mass distributions (effective temperatures) are similar for the $\rho+\omega$ and for the ϕ vector-mesons and smoothly rise from $\approx$ 200 MeV in p-W up to 230 MeV in S-U collisions.

Acknowledgements. This work was supported in part by the portuguese Fundação para a Ciência e Tecnologia.

References

1. M. Jacob, Proceedings of the Symposium on the Quark, the Plasma and Beyond, Bielefeld, Germany, 17–18 May 1996; and references therein
2. J. Rafelski, B. Muller, Phys. Rev. Lett. **48**, 1066 (1982)
3. A. Shor, Phys. Rev. Lett. **54**, 1122 (1985)
4. C. Baglin et al. (NA38 Coll.), Phys. Lett. B **220** 471 (1989); C. Baglin et al. (NA38 Coll.), Phys. Lett. B **255**, 459 (1991)
5. J. Guimarães, Master Thesis, 1996, IST, Universidade Técnica de Lisboa
6. P. Bordalo et al. (NA38 Coll.), Proceedings of the Workshop on Strangeness in Hadronic Matter, S'95, Tuckson (USA), 1995, AIP Press, No. 340, 1995
7. R. Ferreira, Ph.D Thesis, 1992, IST, Universidade Técnica de Lisboa
8. M. Abreu et al. (NA38 Coll.), Phys. Lett. B **368**, 239 (1996); M. Abreu et al. (NA38 Coll.), Phys. Lett. B **368**, 230 (1996)
9. C. Caso et al. (PDG), Eur. Phys. J. C **3**, 1 (1998)
10. C. Quintans, Master Thesis, 1997, IST, Universidade Técnica de Lisboa; C. Quintans, et al. (NA50 Coll.), Proceedings of the Strangeness 2000, SQM'2000 Conference, Berkeley (USA), 2000. J. Phys. G: Nucl. Part. Phys. **27**, 405–412 (2001)
11. R. Mandry, PhD Thesis, 1993, Institut de Physique Nucléaire de Lyon, Université Claude Bernard

12. M. Abreu et al. (NA50 Coll.), Eur. Phys. J. C **14**, 443 (2000)
13. C. Lourenço, Ph.D Thesis, 1995, IST, Universidade Técnica de Lisboa
14. J. Cronin et al., Phys. Rev. D **11**, 3105 (1975)
15. R. Glauber, High energy Collisions Theory in: Lectures in Theoretical Physics, Vol I, Interscience, New York, 1959, p. 315
16. R. Hagedorn, Riv. Nuovo Cimento **6**, 1 (1984)
17. U. Heinz, Nucl. Phys. A **685**, 414 (2001)